

Vietnam Journal of Earth Sciences

https://vjs.ac.vn/index.php/jse



Enhancing potential fields using stable downward continuation and boundary filters: Application to the Central Highlands, Vietnam

Luan Thanh Pham^{1,*}, Saulo P. Oliveira², Long Duc Luu¹, Long Tuan Do¹

Received 16 March 2025; Received in revised form 4 April 2025; Accepted 15 April 2025

ABSTRACT

The stable downward continuation method can enhance low amplitude anomalies and improve the resolution of potential fields. However, this method may be affected by the edge effect. In this paper, we improve the downward continuation results by using the cubic Hermite interpolation to extend data. Our synthetic model shows that the proposed extension can provide better estimates, especially at the edges, than using constant values. We further enhance downward continued data using boundary filters where the boundaries obtained from the downward continued data have a higher resolution. The methods are also applied to interpret RTP magnetic and Bouguer gravity anomalies of the Central Highlands (Vietnam), where the RTP magnetic data are determined from the multiple-stage RTP method, while the Bouguer gravity data are calculated using the Parker formula. The spectral analysis of potential fields reveals the depth of shallow sources in the area of about 1 km, which determines the height of the downward continuation. A new subsurface structural map is established for the Central Highlands from the filtered results of downward continued data, which will be a helpful document for detailed future explorations and geology studies of the area.

Keywords: Downward continuation, cubic Hermite interpolation, boundary filters, Central Highlands (Vietnam).

1. Introduction

Potential field methods usually play an important role in mapping geological structures and mineral deposits (Ekinci and Yiğitbaş, 2012, 2015; Oksum, 2021). A downward continuation can increase the resolution of potential field data. Baranov (1975) developed the formula for downward continuation based on the potential field theory. However, this approach relies highly on the original data's sampling interval and

can only descend to shallow depths. Several methods have focused on the stability of the downward continuation. Fedi and Florio (2002) proposed the integrated second vertical derivative technique based on a Taylor series expansion. Trompat et al. (2003) introduced two new methods: a mild low pass filter and a combination of translation-invariant denoising and Wiener filter. Xu et al. (2007) suggested using the iteration method for downward continuation. Pašteka et al. (2012) used the Tikhonov regularization to provide a stable downward continuation. Zhang et al. (2013) improved the downward continuation using

236

¹University of Science, Vietnam National University, Hanoi, Vietnam

²Department of Mathematics and Graduate Program in Geology, Federal University of Paraná, Curitiba, Brazil

^{*}Corresponding author, Email: luanpt@hus.edu.vn

the Taylor series and iterative method. Zhang et al. (2018) introduced new methods for downward continuation using the mean-value theorem. Tran and Nguyen (2020) recently combined the Taylor series expansion and upward continuation data to provide a stable downward continuation method. The upward continuation used in their method is based on the Fourier transform, which requires that the performing data be prepared before transforms. This preparation usually includes the extension of data to reduce the edge effect. Tran and Nguyen (2020) extended their data using constant values at the edges of the data window. However, this approach does not provide good results at the data edges. In addition, the downward continuation may not be sufficient to outline the source location, as the anomaly amplitudes are heterogeneous.

To solve this issue, some boundary filters have been introduced, which are based upon field derivatives (Abdelrady et al., 2024). The amplitude filters such as the total gradient (Nabighian, 1972), horizontal gradient (Cordell, 1979), gravity gradient tensor (Beiki, 2010), and second horizontal gradient (Tatchum et al., 2011) are usually used in interpreting potential fields. The disadvantage of these filters is that they introduce faint edges for deep sources (Ekinci, 2013; Jorge et al., 2023). Some balanced techniques have been introduced, including the tilt angle (Miller and Singh, 1994), theta (Wijns et al., 2005), and horizontal tilt angle (Cooper and Cowan, 2006) to solve this problem. Since these techniques tend to bring additional boundaries, some high-order filters have also been developed, for example, the tilt angle of the horizontal gradient (Ferreira et al., 2013), horizontal gradient-based edge detector (Pham et al., 2023), modified horizontal gradient (Ai et al., 2024a), hyperbolic tangent function (Ai et al., 2024b), Elliott function (Alvandi et al., 2024) and modified Gudermannian function (Alvandi et al., 2025). Some authors (e.g., Zhang et al., 2015; Ma et al., 2016; Nasuti et al., 2018; Nasuti and Nasuti, 2019; Kafadar

and Oksum, 2024) have also developed other filters to improve the boundary resolution. Recently, case studies have illustrated the usefulness of the filters in extracting structural features (Saibi et al., 2012a, b; Oruç, 2014; Narayan et al., 2016, 2021; 2024; Altınoğlu 2021; 2023; Sahoo et al., 2022a, b; Kamto et al., 2023; Oruç and Balkan, 2023; Pham et al., 2024; Saada et al., 2025).

In this paper, we further enhanced downward continued data using boundary filters such as the theta, horizontal tilt angle, tilt angle of the horizontal gradient, and horizontal gradient-based edge detector. We also improved the downward continuation performance using the cubic Hermite interpolation. Gravity and magnetic maps of the Central Highlands (Vietnam) are also interpreted for the first time using these methods.

2. Methods

2.1. Downward continuation

Downward continuation is a potential field transformation that changes the observation height of the data to a lower altitude, increasing its resolution. This method amplifies high-frequency content, originating from shallow sources and data noise. Thus, although it can be easily implemented in the wavenumber domain, a stabilizing strategy is often needed for its practical usage.

We consider a stable implementation based on the Taylor series expansion proposed by Tran and Nguyen (2020). The derivatives in the expansion are approximated by equally-spaced finite differences and simultaneously computed by solving a linear system. As a result, the derivatives are approximately written as linear combinations of the data upward-continued to equally-spaced heights. When these expressions are substituted into the Taylor series expansion, we obtain a downward continuation formula of the following type:

$$F(x, y, z + \Delta z) = 9F(x, y, z) - 36F(x, y, z - \Delta z) + 84F(x, y, z - 2\Delta z) - 126F(x, y, z - 3\Delta z) + 126F(x, y, z - 4\Delta z) - 84F(x, y, z - 5\Delta z) + 36F(x, y, z - 6\Delta z) - 9F(x, y, z - 7\Delta z) + F(x, y, z - 8\Delta z).$$
(1)

To further improve the performance of Eq. (1), we extend data of the study area using the cubic Hermite interpolation instead of using constant values at the edges like the computations of Tran and Nguyen (2020). This interpolation ensures smooth transitions based on edge values and gradients. The data extension employed in this manuscript follows the strategy from the taper2d script from the Potensoft code (Arrsoy and Dikmen, 2011; and see also Cooper and Cowan, 2008). Fig. 1 shows a simple example of the constant and cubic Hermite interpolation-based extensions. This figure illustrates that the data is extended in each spatial direction with a cubic function that connects to both data endpoints. We can first extend all data rows and subsequently extend all data columns.

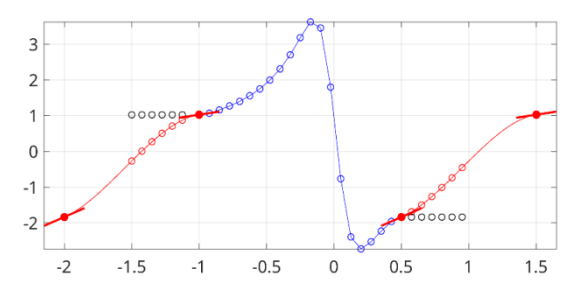


Figure 1. 1-D view of the data extensions. Blue circles represent the data, black circles correspond to the constant extension, and red circles represent

the extended data by the cubic Hermite interpolation. The data values at the endpoints and their slopes (represented as filled red circles and thick line segments) are employed to calculate the cubic function (red thin curve) that generates the extended data

For instance, let $F = [f_0, f_1, ..., f_n]$ be a data row, and suppose we want to extend this row with k points. We select the cubic function p(x) such that,

$$p(x_1) = f_n p(x_2) = f_0 p'(x_1) = df_n p'(x_2) = df_0,$$
 (2)

where $x_1 = 0$, $x_2 = 2k + 1$, and df_0 and df_n represent the slopes of F at the endpoints. Afterwards, we evaluate p(x) at x = 1,...,k to extend the data to the right of f_n , and evaluate p(x) at x = k + 1,...,2k to the extend the data to the left of f_0 .

By writting $p(x) = c_0 + c_1x + c_2x^2 + c_3x^3$, it follows from Eq. (2) that $c_0, ..., c_3$ can be found by solving the linear system.

$$c_{0} + c_{1}x_{1} + c_{2}x_{1}^{2} + c_{3}x_{1}^{3} = f_{n}$$

$$c_{0} + c_{1}x_{1} + c_{2}x_{1}^{2} + c_{3}x_{1}^{3} = f_{0}$$

$$0 + c_{1} + 2c_{2}x_{1} + 3c_{3}x_{1}^{2} = df_{n}$$

$$0 + c_{1} + 2c_{2}x_{1} + 3c_{3}x_{1}^{2} = df_{0}.$$
(3)

2.2. Boundary filters

Downward continuation can significantly increase the resolution of potential field maps but may not be sufficient to locate the causative sources, as the amplitudes of their anomalies may be heterogeneous. In this situation, high-amplitude anomalies predominate, while low-amplitude anomalies may be ignored.

Several filters proposed in the literature can equalize anomalies. Perhaps the most classical ones are the tilt angle (Miller and Singh, 1994),

$$TA = atan \frac{\frac{\partial F}{\partial z}}{\sqrt{\left(\frac{\partial F}{\partial x}\right)^2 + \left(\frac{\partial F}{\partial y}\right)^2}},$$
 (4)

the TM (Wijns et al., 2005),

$$TM = a\cos\frac{\sqrt{\left(\frac{\partial F}{\partial x}\right)^2 + \left(\frac{\partial F}{\partial y}\right)^2}}{\sqrt{\left(\frac{\partial F}{\partial x}\right)^2 + \left(\frac{\partial F}{\partial y}\right)^2 + \left(\frac{\partial F}{\partial z}\right)^2}}$$
(5)

and the horizontal tilt angle (Cooper and Cowan, 2006),

Luan Thanh Pham et al.

$$TDX = atan \frac{\sqrt{\left(\frac{\partial F}{\partial x}\right)^2 + \left(\frac{\partial F}{\partial y}\right)^2}}{\left|\frac{\partial F}{\partial z}\right|}.$$
 (6)

High-order versions of the tilt angle filter have been developed by combining it with additional filters. An example of such a filter is the tilt angle of the horizontal gradient (Ferreira et al., 2013):

$$TAHG = atan \frac{\frac{\partial THG}{\partial z}}{\sqrt{\left(\frac{\partial THG}{\partial x}\right)^2 + \left(\frac{\partial THG}{\partial y}\right)^2}},$$
 (7)

$$THGED = atan \frac{\frac{\partial THG}{\partial z} - \sqrt{\left(\frac{\partial THG}{\partial x}\right)^2 + \left(\frac{\partial THG}{\partial y}\right)^2}}{\sqrt{\left(\frac{\partial THG}{\partial x}\right)^2 + \left(\frac{\partial THG}{\partial y}\right)^2 + \left(\frac{\partial THG}{\partial z}\right)^2}}.$$
(9)

3. Results

3.1. Synthetic model

We created a synthetic model that included two prisms to consider the effectiveness of the methods. The prisms and their gravity anomaly are presented in Figs: 2a and 2b. As shown in Fig. 2b, we cannot determine the location of body B1 from the original gravity anomaly. Fig. 3a depicts the gravity anomaly of the model at z = -5 km. Figs. 3b and 3c show the results with downward continuation by 5 km of data in Fig. 2b using the Tran-Nguyen extension and proposed approach. As in Fig. 3a, one can see that the downward continuation results enhanced the gravity anomaly, so they provide information on the location of body B1. Comparing figures, we can see that both approaches provide similar results (Figs. 3b and 3c) with theoretical values (Fig. 3a). To know the difference between anomalies in Fig. 3a and anomalies in Figs. 3b and 3c, we considered a profile along the E-W direction (the white line in Fig. 3a), shown in Fig. 3d. Our approach provides better results than the original where THG is given by (Cordell, 1979):

$$THG = \sqrt{\left(\frac{\partial F}{\partial x}\right)^2 + \left(\frac{\partial F}{\partial y}\right)^2}.$$
 (8)

Another approach is to use the inverse tangent of generalized ratios that do not necessarily represent the tilt angle of the anomalous field or a transformed field but enhance the edge detection, preserving amplitude equalization, as proposed by Pham et al. (2024):

approach, especially at the edges. The root mean square error between the theoretical field (Fig. 3a) and the result from the Tran-Nguyen method (Fig. 3b) is 0.1528 mGal, while the error from our approach is only 0.0878 mGal.

In Fig. 4, we further enhanced the gravity and downward continued gravity anomalies using some boundary filters. Figs. 4a-4d shows the outputs of the TM, TDX, TAHG, and THGED of the gravity anomaly, respectively. It can be seen that the TM and TDX methods are effective in mapping body B2, but they do not show the boundaries of the shallow body B1. The TAHG and THGED methods can map all the boundaries. However, the signals over the boundaries of body B1 are faint. The TM, TDX, TAHG and THGED outputs of the downward continued gravity anomaly are presented in Figs. 4e-4f, respectively. In this case, the filtered maps show the boundaries of body B1 more clearly than the results of the gravity anomaly. In addition, the boundaries in Figs. 4e-4f have a higher resolution compared to those from Figs. 4a-4d.

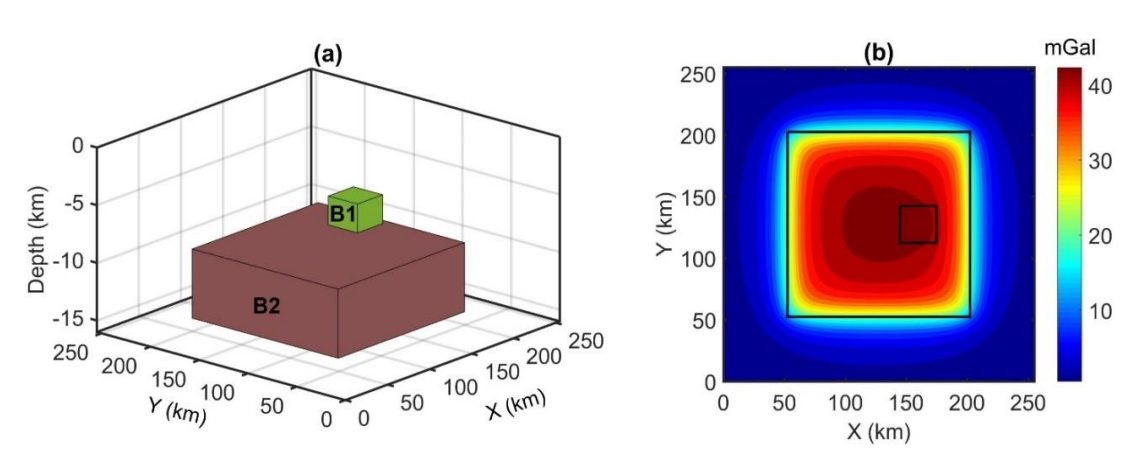


Figure 2. (a) Synthetic model, (b) Gravity anomalies of the model

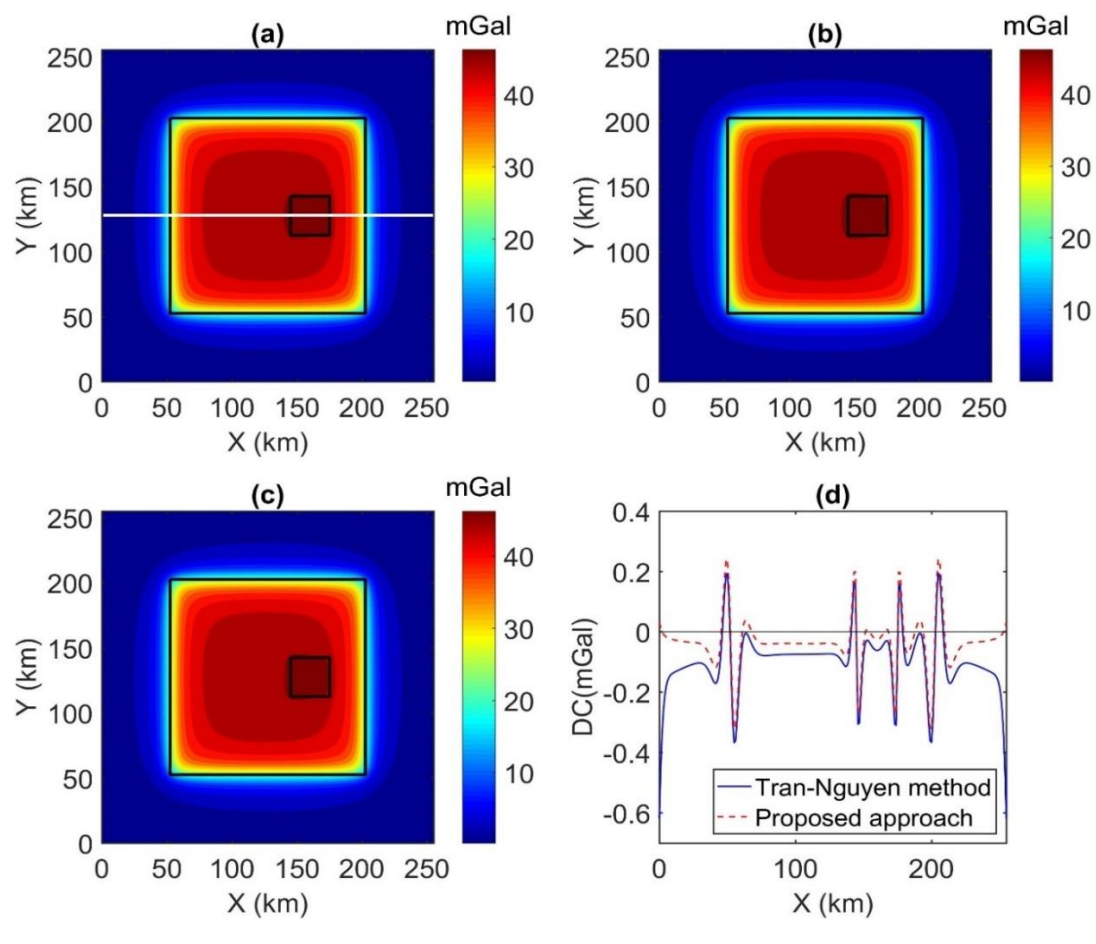


Figure 3. (a) Gravity anomalies at z = -5 km, (b) Downward continuation of data in Fig. 2b using the Tran-Nguyen method, (c) Downward continuation of data in Fig. 2b using the proposed approach, (d) Differences between anomalies in Fig. 3a and anomalies in Figs. 3b and 3c along the E-W profile (Fig. 3a)

Luan Thanh Pham et al.

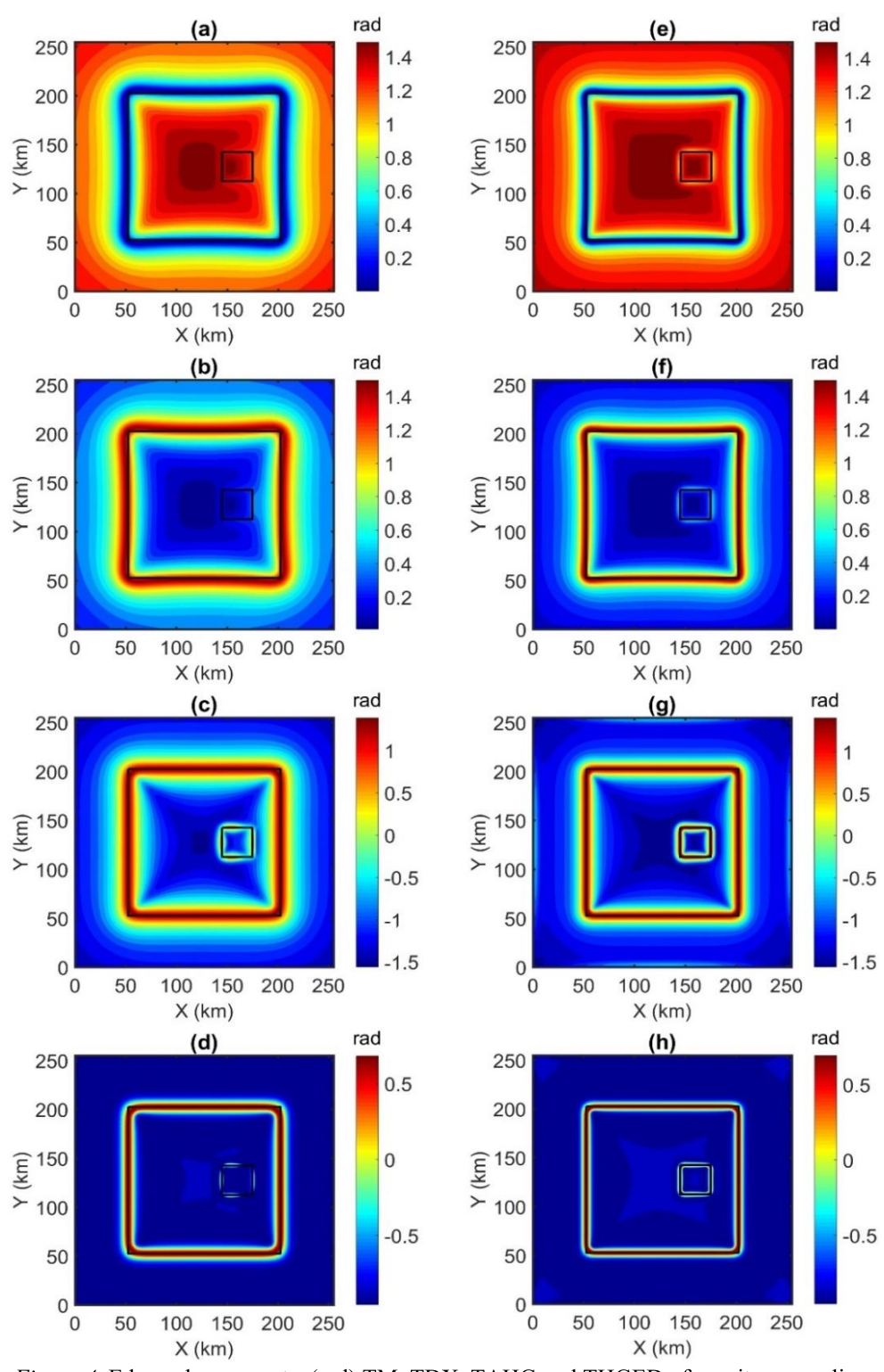


Figure 4. Edge enhancements: (a-d) TM, TDX, TAHG and THGED of gravity anomalies, (e-h) TM, TDX, TAHG and THGED of downward continued gravity anomalies

3.2. Real application

In this section, we used the methods to interpret magnetic and gravity data of the Central Highlands, Vietnam (Fig. 5). It is Indochina located in the Block, microcontinental fragment that has been shaped by multiple tectonic events related to the assembly and breakup of supercontinents, as well as the India-Eurasia collision. The Central Highlands consist of a series of plateaus formed primarily on basalt bedrock, with elevations ranging from 500 to 1,500 meters above sea level (Hướng et al., 2023). Basalt formations, Precambrian basement, and sedimentary and Metamorphic rocks dominate the area's geology. The geological map of the study region is depicted in Fig. 5 (Nong et al., 2022). One can see that most of the area is covered by the Neogene-Quaternary basaltic and Mesozoic igneous rocks and Jurassic-Cretaceous sediments (Fig. 5). There are some studies based on magnetic and gravity data for determining structures in the area. Pham et al. (2018) used magnetic data with a resolution of 4 km from the Coordinating Committee for Geoscience Programmes in Asia to map the magnetic boundaries in the western part of the study region. Vu et al. (2021) mapped the Moho lithosphere-asthenosphere boundaries for the whole of Vietnam from gravity data of the GEOID LSC model. Recently, using gravity data, Liu et al. (2023) mapped multi-phase tectonic boundaries in the Indo-China Peninsula. However, these studies only provided regional structures.

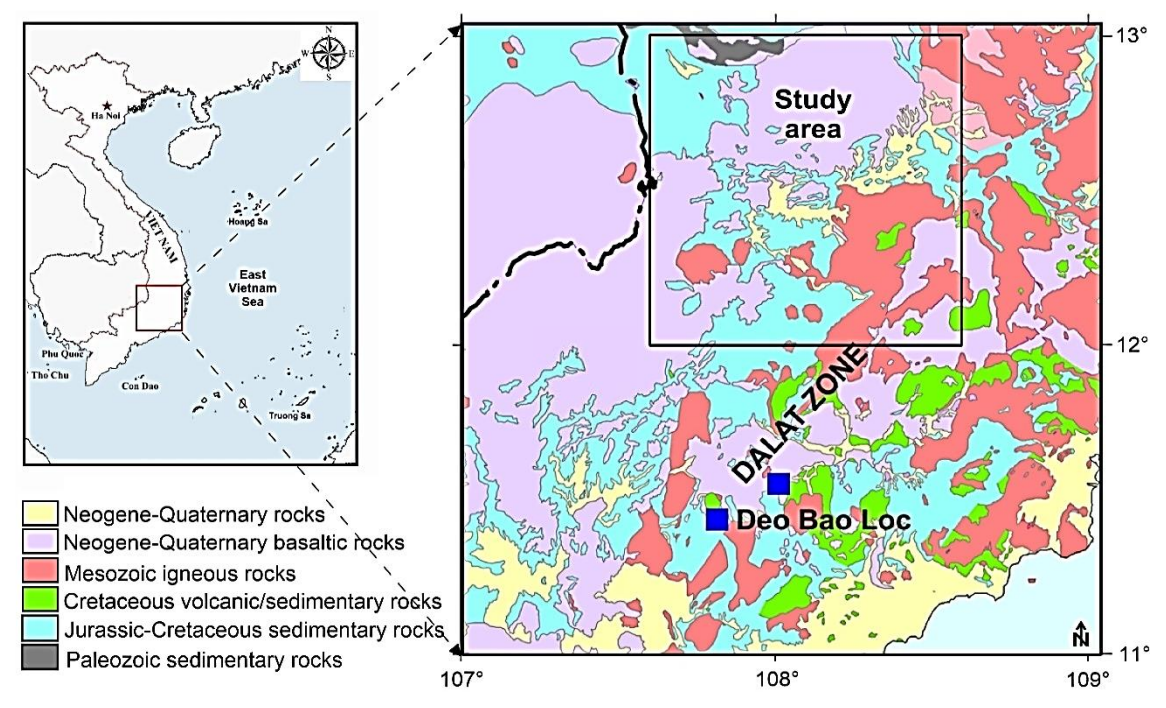


Figure 5. Geological map of the Central Highlands and adjacent areas (Nong et al., 2022)

High-resolution magnetic data (Fig. 6a) of the study area are provided by the Department of Geology and Minerals of Vietnam. In contrast, Bouguer gravity data (Fig. 6d) are calculated from the Free-air data (Fig. 6b) of the global gravity model of Sandwell et al.

(2014). This model uses EGM2008 data for land areas. A recent review by Narayan et al. (2023) showed that the EGM2008 model compares favorably with the later models. Magnetic data were transformed to the pole using the multiple-stage RTP method of Stewart (2019) with an inclination of 13.71° and a declination of -0.97° (Fig. 6b). Here, we performed RTP in two equal steps, rotating the field by 38.15° in each step. This is the

same as doing a single RTP calculation for an inclination of 51.85°. For this reason, the multiple-stage RTP method can provide stable results, as shown in Fig. 6b, with values ranging from -429.04 to 305.65 nT. We used the Parker method to compute the gravity correction with an average continental crust density of 2.67 g/cm³. The gravity map is characterized by negative anomalies changing from -91.62 to -19.89 mGal (Fig. 6d).

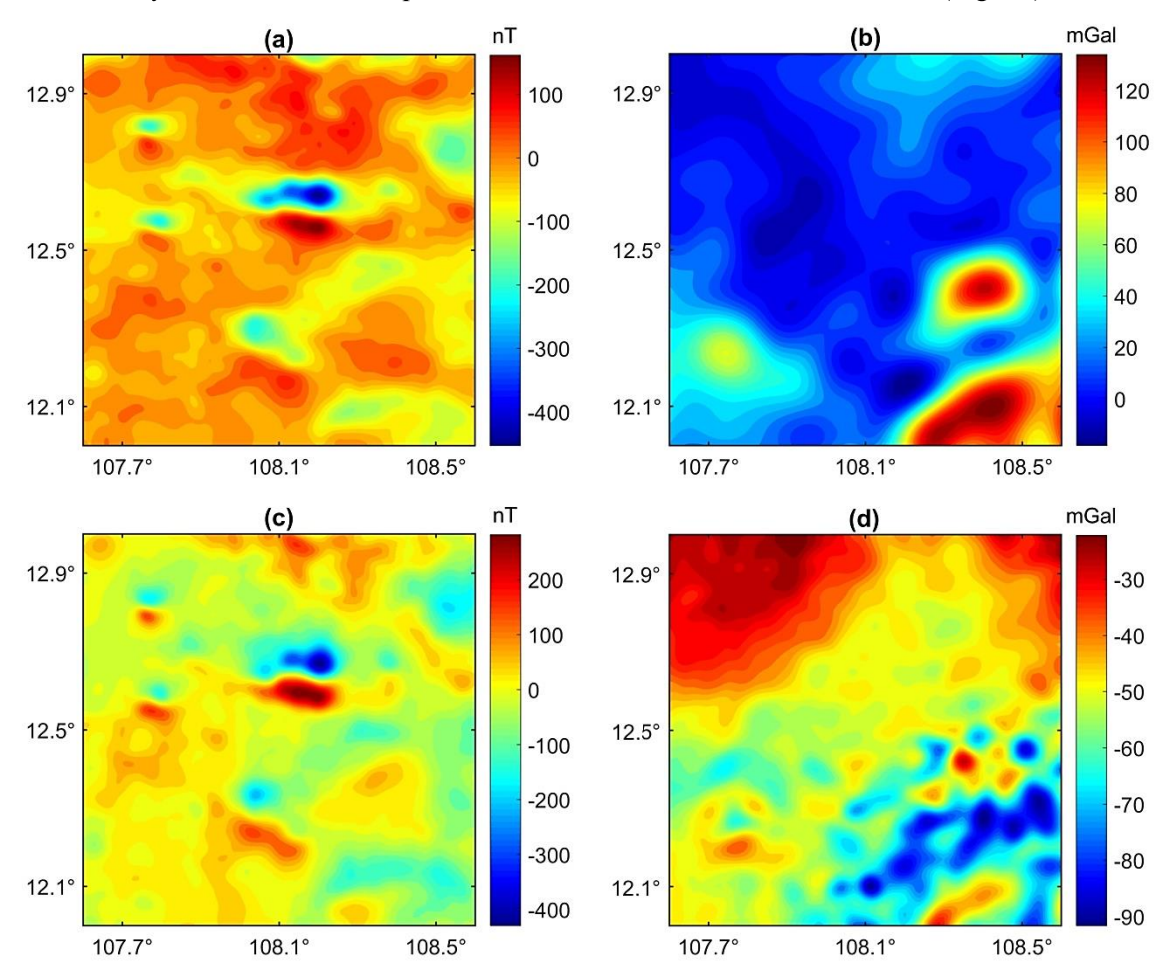


Figure 6. Magnetic and gravity data from the Central Highlands: (a) Magnetic anomalies, (b) Free-air gravity anomalies, (c) RTP magnetic anomalies, (d) Bouguer gravity anomalies. The grid sampling of the magnetic and gravity data were 0.5 km and 1.1 km, respectively

We estimated the depth levels of magnetic and gravity sources using the radial power spectrum to determine the height of the downward continuation for the actual application. The spectral analysis of RTP magnetic data in Fig. 6b provides depths of 3.9,

2.5, and 1 km for deep, average, and shallow magnetic sources, respectively (Fig. 7a). For Bouguer data, we obtain the depth levels of 6.5, 4.7 and 2 km from the power spectrum (Fig. 7b). Therefore, it is reasonable to use a downward continuation height of 1 km for magnetic and gravity data in the study area. The downward continuation of RTP magnetic and Bouguer data to 1 km are shown in Figs:

8a and 8b using the proposed data extension, respectively. The downward continued magnetic and gravity maps show larger values than the original maps, which range from -635.68 to 455.27 nT and -110.85 to -5.99 mGal, respectively. The improvement in resolution is clearly visible by comparing the downward continued maps (Figs. 8a and 8b) with the original maps (Figs. 7b and 7c).

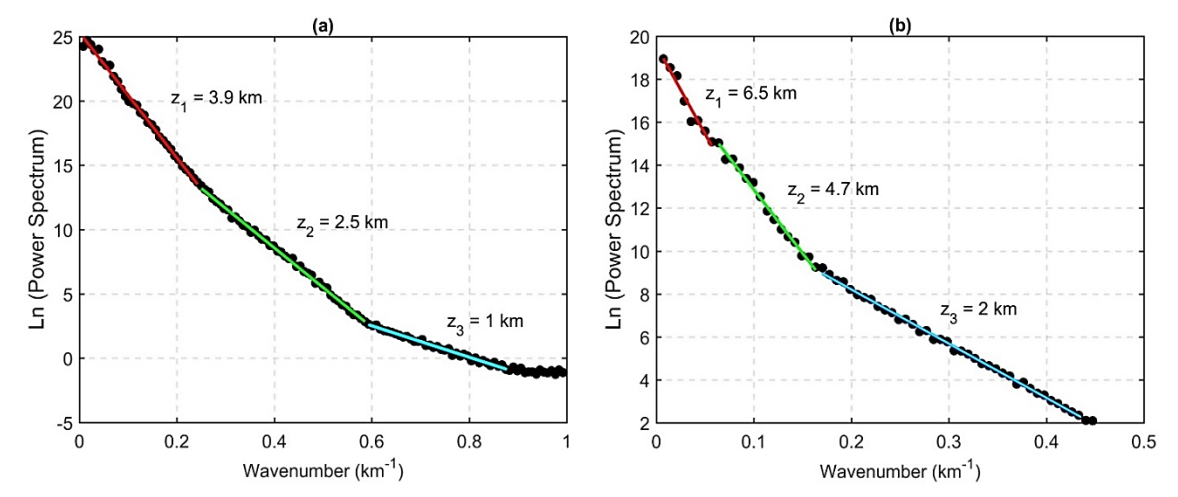


Figure 7. The power spectrums of RTP magnetic anomalies (a) and Bouguer gravity anomalies (b)

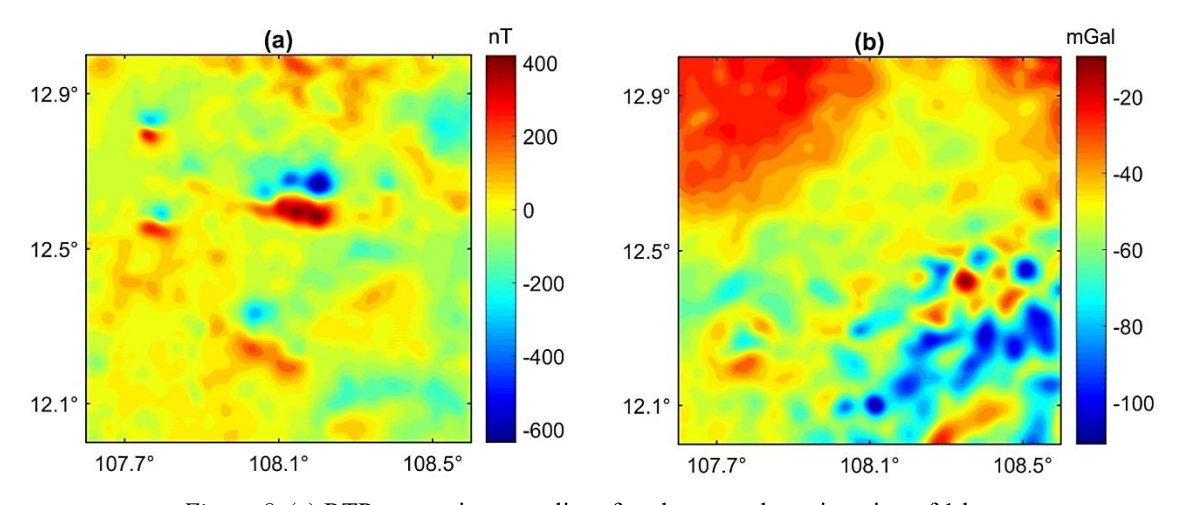


Figure 8. (a) RTP magnetic anomalies after downward continuation of 1 km, (b) Bouguer gravity anomalies after downward continuation of 1 km

The TM, TDX, TAHG, and THGED filters were applied to downward continued maps to map structural features of the Central

Highlands. Figs. 9a-9d shows the TM, TDX, TAHG, and THGED of downward continued magnetic data, respectively. The boundaries are

determined by minimum contours in the TM map and maxima in the TDX map. It can be observed that the boundaries in the TM and TDX maps are connected to adjacent boundaries. The TAHG and THGED maps provide similar outputs. The peaks in these maps are located over the magnetic boundaries. Although both the TAHG and THGED methods effectively locate many magnetic boundaries, the THGED method can provide the shaper boundaries. The TM, TDX, TAHG, and THGED results of downward continued

gravity data are shown in Figs. 10a-10d, respectively. Like the magnetic case, the TM and TDX maps also show the connected boundaries. The TAHG and THGED detectors are good at finding many density boundaries, but the THGED approach shows the shaper boundaries. By interpreting the THGED outputs, we determined the magnetic and density boundaries as shown in Figs. 11a and 11b, respectively. These boundaries may be related to potential faults or contacts in the Central Highlands.

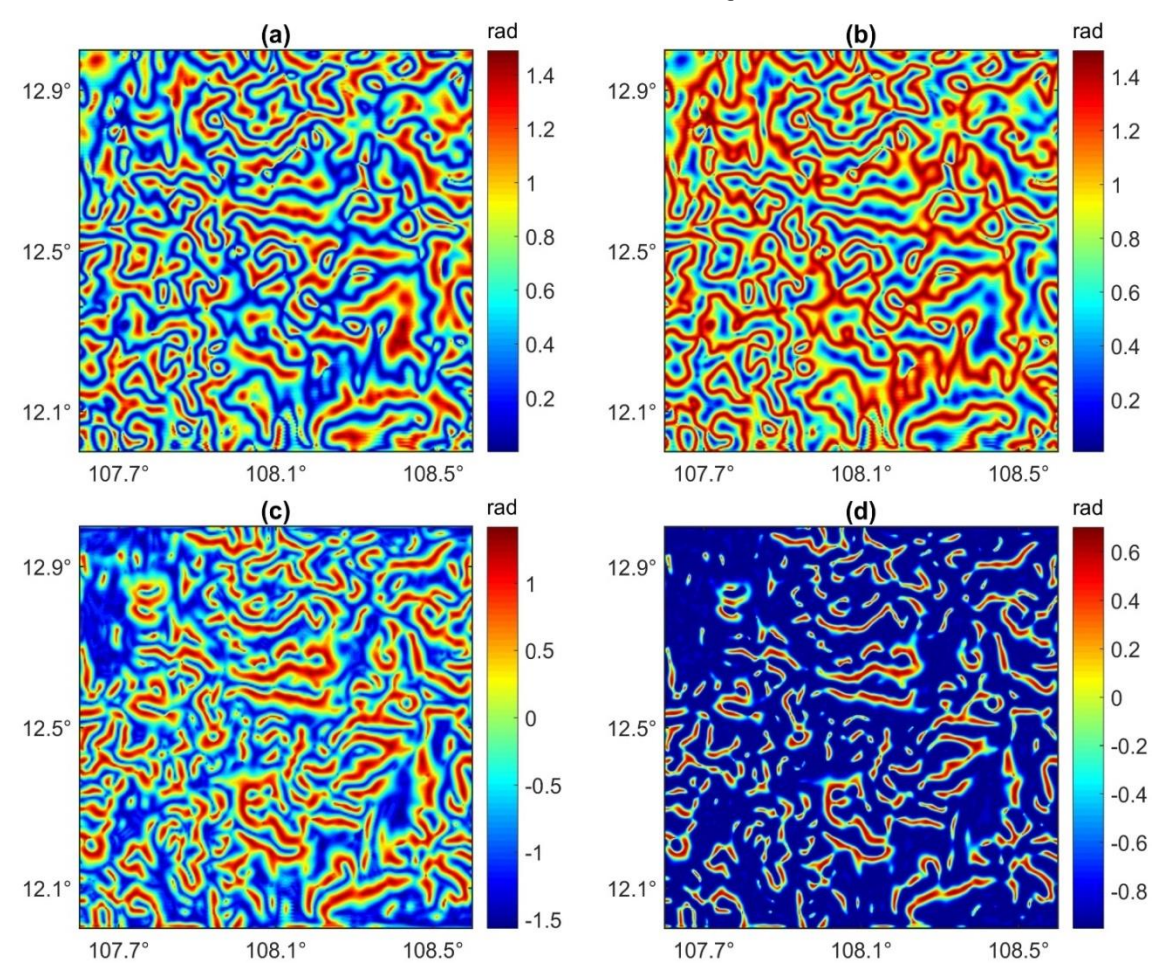


Figure 9. Edge enhancements of RTP magnetic anomalies after downward continuation of 1 km: (a) TM, (b) TDX, (c) TAHG, (d) THGED

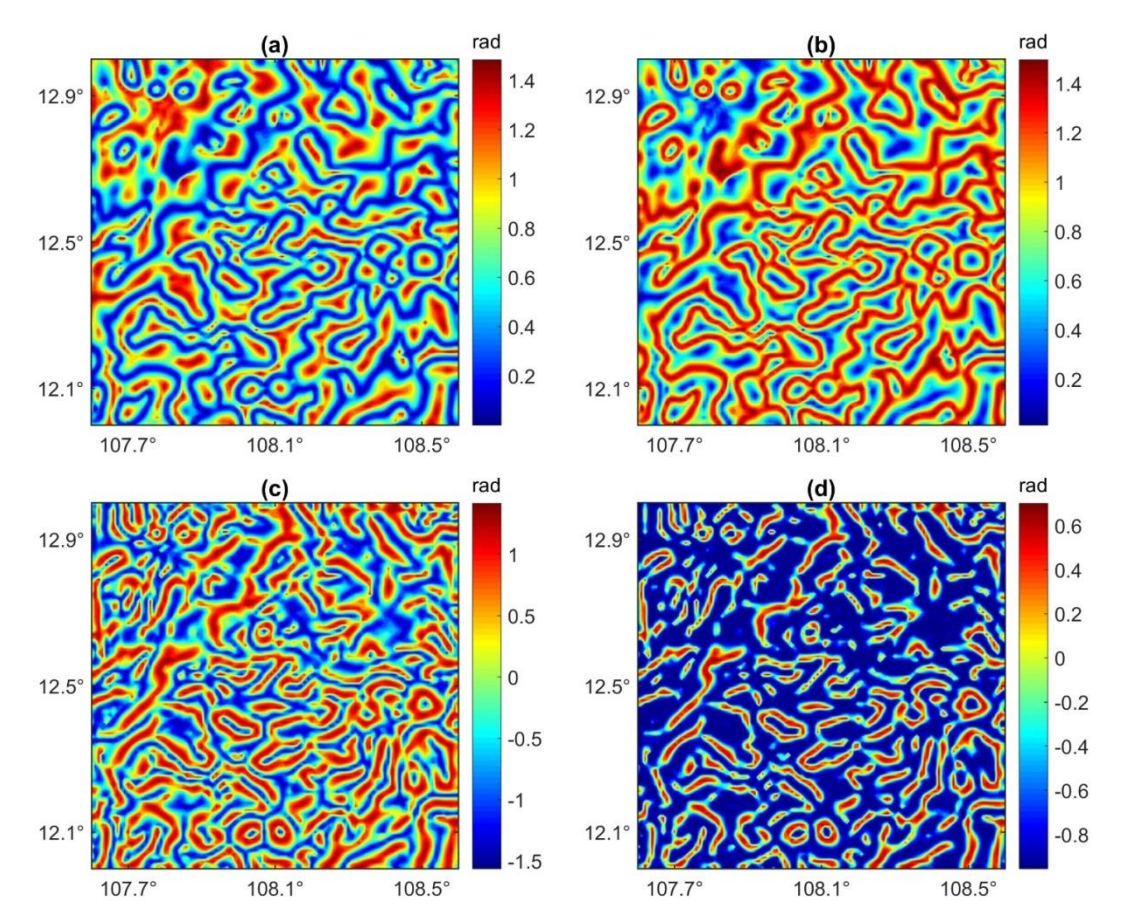


Figure 10. Edge enhancements of Bouguer gravity anomalies after downward continuation of 1 km: (a) TM, (b) TDX, (c) TAHG, (d) THGED

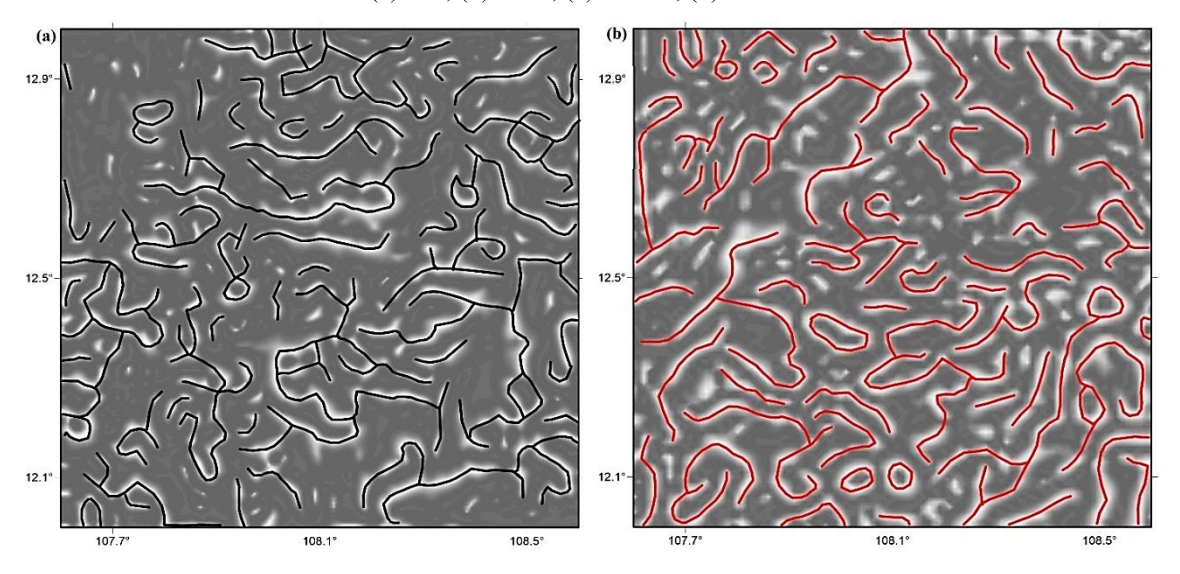


Figure 11. (a) Magnetic boundaries from the THGED of downward continued RTP data, (b) Gravity boundaries from the THGED of downward continued Bouguer data

Luan Thanh Pham et al.

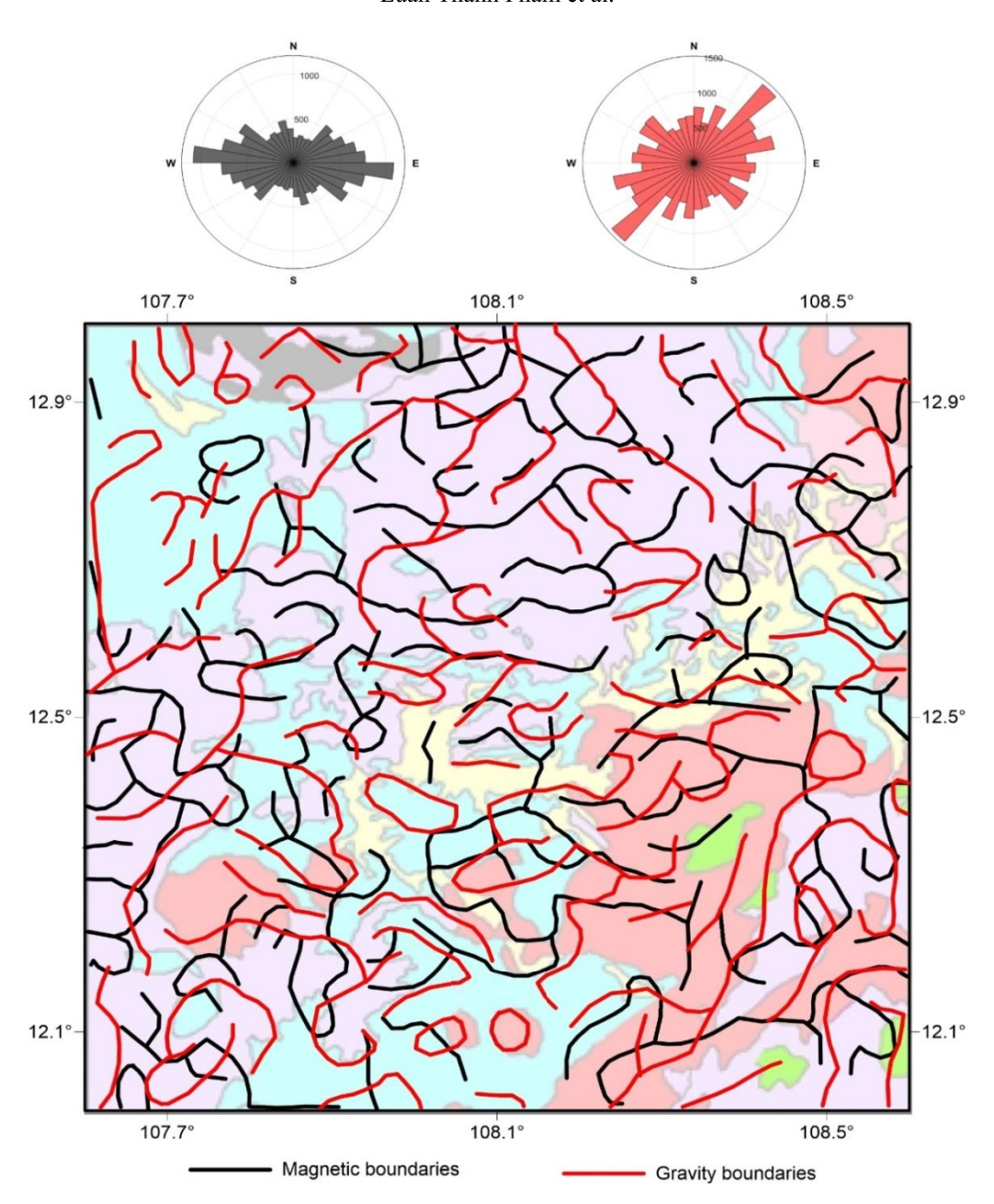


Figure 12. Structural map of the Central Highlands

5. Discussions

The downward continuation method of Tran and Nguyen (2020) is a stable approach for enhancing potential field data. Due to the edge effect when using the Fourier transforms, Tran and Nguyen (2020) extended data employing constant values at the edges.

This can provide better results compared to the calculation without extension. However, the continual extension approach does not represent the data trends well. Our model study showed that the use of the cubic Hermite interpolation for extending data can provide better results than the constant extension, especially at the edge regions (Fig. 3). The weak anomalies due to the shallow sources with slight density contrast have been accurately and enhanced using our approach (Figs. 3c and 3d). The application of boundary filters to downward continued data also showed the boundaries of the weak anomalies more clearly than those from the original data (Fig. 4). The determined boundaries also have a higher resolution (Fig. 4).

We also applied our approach to enhance the magnetic and gravity data of the Central Highlands. As can be seen from Figs. 8a and 8b, the features in the original RTP magnetic and Bouguer maps are better displayed in the downward continuation maps. Therefore, downward continuation maps can improve the resolution of later interpretation results. Figs. 9 and 10 show that the presented approach can provide reliable boundary determination results even using first and second-order derivative-based filters.

The TM and TDX filters generate faint signals over the boundaries of the shallow source B1 (Figs. 4a, 4b, 4e, and 4f), and lineaments in the TM and TDX maps are connected (Figs. 9a, 9b, 10a, and 10b). The TAHG and THGED filters can accurately detect all boundaries without false information. The THGED filter detects the lineaments better than other filters among the boundary filters. For this reason, established a new subsurface structural map (Fig. 12) for the Central Highlands using the outputs of the THGED filter (Figs. 11a and 11b). The rose diagrams of magnetic (black) and gravity (red) boundaries are also added to this map to indicate the directional trends of these boundaries. The TAHG maps also confirm the structural features in Fig. 12. The structural map reveals the existence of many geological bodies that are obscured by the Neogene-Quaternary basaltic and Mesozoic igneous rocks, as well as Jurassic-Cretaceous sediments in the Central Highlands. The magnetic and gravity boundaries reflect a complex tectonic history, with overlapping compression, extension, and strike-slip movement phases.

Magnetic lineaments are more sensitive to shallow crustal features, such as faults or igneous intrusions with magnetic minerals, while gravity lineaments reflect deeper density contrasts. Indeed, our spectral analysis showed the magnetic sources in the area are shallower than 3.9 km (Fig. 7a), while the deepest gravity sources are found at an average depth of 6.5 km (Fig. 7b). As shown 12, the magnetic boundaries Fig. demonstrate the dominance of the E-W oriented trend. However, the gravity interpretation shows the predominant NE-SW trend with some secondary directions, such as NW-SE ENE and WSW. According to Phach and Anh (2018), the NE-SW trend dominates the tectonic faults in the southern region of the Central Highlands. This agrees with the dominant NE-SW trend in our structural map (Fig. 12). The gravity structures also correlate well with the trend of the tectonic fractures determined by Viet et al. (2016) in the Central Highlands. One can see from Fig. 12 that the magnetic and gravity boundaries complement each other. It should be noted, nevertheless, that while magnetic data are obtained from airborne surveys, gravity data are satellite measurements. As a result, the frequency of these data contents shouldn't comparable. Difference from the previous magnetic and gravity studies (i.e., Pham et al., 2018; Liu et al., 2023), our study provided additional information on subsurface structures in the Central Highlands, as shown in Fig. 12. The existence of such formations only can infer from geophysical mapping, while geological study alone cannot determine their existence. Thus, the structural map established from our interpretation will be useful for more detailed geophysical and geological studies in the Central Highlands.

6. Conclusions

The downward continuation performance has been improved by using the cubic Hermite interpolation to extend data instead of the constant extension. Data from downward continued were also further enhanced using boundary filters. The methods were estimated using the synthetic model, where the proposed extension can provide more accurate estimates, especially at the edges. The results also showed that applying boundary filters to downward continued data can outline all the boundaries with a higher resolution than the original data. We also used the methods to interpret RTP magnetic and Bouguer gravity anomalies of the Central Highlands (Vietnam), where the downward continuation height of 1 km was obtained from the spectral analysis. The results contributed establishing the structural map of the Central Highlands, which is a handy document for more detailed geophysical and geological studies.

Acknowledgments

This research was funded by the research project QG.23.64 of Vietnam National University, Hanoi. We thank Danielle Rocha Gonçalves for revising the data extension procedure. S.P. Oliveira is grateful to the Brazilian agency CNPq (316376/2021-3).

References

- Abdelrady M., Pham L.T., Mohamed A., Alarifi S.S., Duong V.H., Mohammed M.A.A., 2024. Application of the new edge filters of aeromagnetic data to detect the subsurface structural elements controlling the mineralization in the Barramiya area, Eastern Desert of Egypt. J. King Saud Univ. Sci., 36(11), 103539.
- Ai H., Deniz Toktay H., Alvandi A., Pašteka R., Su K., Liu Q., 2024a. Advancing potential field data analysis: the modified horizontal gradient amplitude method (MHGA). Contrib Geophys Geodesy, 54(2), 119–143.

- Ai H., Ekinci Y.L., Alvandi A., Deniz Toktay H., Balkaya Ç., Roy A., 2024b. Detecting edges of geologic sources from gravity or magnetic anomalies through a novel algorithm based on hyperbolic tangent function. Turk. J. Earth Sci., 33(6), 6.
- Altınoğlu F.F., 2021. Structural interpretation of Buldan region in Western Anatolia by using magnetic and gravity data. ANAS Transactions Earth Sciences, 1, 47–55.
- Altınoğlu F.F., 2023. Mapping of the Structural Lineaments and Sedimentary Basement Relief Using Gravity Data to Guide Mineral Exploration in the Denizli Basin. Minerals, 13(10), 1276.
- Alvandi A., Ardestani V.E., Motavalli-Anbaran S.-H., 2024. Novel Detectors Based on the Elliott Function for Mapping Potential Field Data: Application to Aeromagnetic Data from Indiana, United States. Ann. Geoph., 67, 6.
- Alvandi A., Ardestani V.E., Motavalli-Anbaran S.-H., 2025. Enhancement of the total horizontal gradient of potential field data using the Modified Gudermannian Function (MGTHG): application to aeromagnetic data from Georgia, USA. Bull. Geophys. Oceanogr., 66, 73–94.
- Arisoy M.O., Dikmen U., 2011. Potensoft: MATLAB-based software for potential field data processing, modeling and mapping. Comput. Geosci., 37, 935–942.
- Baranov W., 1975. Potential fields and their transformation in applied geophysics. Gebruder Borntraeger, Berlin-Stuttgart.
- Beiki M., 2010. Analytic signals of gravity gradient tensor and their application to estimate source location. Geophysics, 75(6), 159–174.
- Cordell L., 1979. Gravimetric expression of graben faulting in Santa Fe Country and the Espanola Basin. In 30th Field Conference New Mexico. New Mexico Geological Society Guidebook; New Mexico Geological Society: Socorro, NM, USA, 59–64.
- Cooper G.R.J., Cowan D.R., 2006. Enhancing potential field data using filters based on the local phase. Comput. Geosci., 32(10), 1585–1591.
- Cooper G.R.J., Cowan D.R., 2008. Edge enhancement of potential field data using normalized statistics. Geophysics, 73(3), H1–H4.
- Ekinci Y.L., Ertekin C., Yiğitbaş E., 2013. On the effectiveness of directional derivative based filters

- on gravity anomalies for source edge approximation: synthetic simulations and a case study from the Aegean graben system (Western Anatolia, Turkey). J. Geophys. Eng., 10(3), 035005.
- Ekinci Y.L., Yiğitbaş E., 2012. A geophysical approach to the igneous rocks in the Biga Peninsula (NW Turkey) based on airborne magnetic anomalies: Geological implications. Geodin. Acta, 25, 267–285.
- Ekinci Y.L., Yiğitbaş E., 2015. Interpretation of gravity anomalies to delineate some structural features of Biga and Gelibolu peninsulas, and their surroundings (northwest Turkey). Geodin. Acta, 27(4), 300–319.
- Fedi M., Florio G., 2002. A stable downward continuation by using ISVD method. Geophys. J. Int., 151, 146–156.
- Ferreira F.J.F., de Souza J., Bongiolo A.B.S., de Castro L.G., 2013. Enhancement of the total horizontal gradient of magnetic anomalies using the tilt angle. Geophysics, 78(3), J33–J41.
- Hướng N.-V., Unkel I., Dương N.-T., Thái N.-Đình, Đỗ T.Q., Đặng X.T., Nguyễn T.H., Đinh X.T., Nguyễn T. Ánh N., Nguyễn H Q., Đào T.H., Nguyễn T.H.T., Phạm L.T.N., Lê L.A., Vũ V.H., Ojala A.E., Schimmelmann A., Sauer P., 2023. Paleoenvironmental potential of lacustrine sediments in the Central Highlands of Vietnam: a review on the state of research. Vietnam J. Earth Sci., 45(2), 164–182.
- Kafadar O., Oksum E., 2024. Enhanced dip angle map using Kuwahara and Gaussian filters: an example from Burdur region, Türkiye. Turk. J. Earth Sci., 33(4), 395–406.
- Kamto P.G., Oksum E., Lemotio W., Kamguia J., 2023. Structural mapping of the Goulfey-Tourba (West and Central African Rift) sedimentary basin using high-resolution gravity data. Earth Sci. Res. J., 239–249.
- Liu J., Wang X., Suo Y., Li S., Zhou J., 2023. A robust high-resolution potential-field edge detection filter with its application in the Indo-China Peninsula. Tectonophysics, 868, 230109.
- Ma G., Huang D., Liu C., 2016. Step-edge detection filters for the interpretation of potential field data. Pure Appl. Geophys., 173 (3), 795–803.
- Miller H.G., Singh V., 1994. Potential field tilt a new concept for location of potential field sources. J. Appl. Geoph., 32, 213–217.

- Nabighian M.N., 1972, The analytic signal of two-dimensional magnetic bodies with polygonal cross-section: Its properties and use of automated anomaly interpretation: Geophysics, 37, 507–517. Doi: 10.1190/1.1440276.
- Narayan S., Sahoo S.D., Pal S.K., Kumar U., Pathak V.K., Majumdar T.J., Chouhan A., 2016. Delineation of structural features over a part of the Bay of Bengal using total and balanced horizontal derivative techniques. Geocarto Int., 32, 351–366.
- Narayan S., Kumar U., Pal S.K., Sahoo S.D., 2021. New insights into the structural and tectonic settings of the Bay of Bengal using high-resolution earth gravity model data. Acta Geophys., 69, 2011–2033.
- Narayan S., Sahoo S.D., Pal S.K., Kumar U., 2023. Comparative evaluation of five global gravity models over a part of the Bay of Bengal. Advances in Space Research, 71(5), 2416–2436.
- Narayan S., Kumar U., Sahoo S.D., Pal S.K., 2024. Appraisal of lineaments patterns and crustal architectures around the Owen fracture zone, Arabian Sea, using global gravity model data. Acta Geophys., 72, 29–48.
- Nasuti Y., Nasuti A., 2018. NTilt as an improved enhanced tilt derivative filter for edge detection of potential field anomalies. Geoph. J. Int., 214(1), 36–45.
- Nasuti Y., Nasuti A., Moghadas D., 2019. STDR: a novel approach for enhancing and edge detection of potential field data. Pure Appl. Geophys., 176(2), 827–841.
- Nong A.T., Hauzenberger C.A., Gallhofer D., Skrzypek E., Dinh S.Q., 2022. Geochemical and zircon U-Pb geochronological constraints on late Mesozoic Paleo-Pacific subduction-related volcanism in southern Vietnam. Miner Petrol, 116, 349–368.
- Oksum E., 2021. Grav3CH_inv: A GUI-based MATLAB code for estimating the 3-D basement depth structure of sedimentary basins with vertical and horizontal density variation. Comput. Geosci., 155, 104856.
- Oruç B., 2014. Structural interpretation of southern part of western Anatolian using analytic signal of the second order gravity gradients and discrete wavelet transform analysis. J. Appl. Geophys., 103, 82–98
- Oruç B., Balkan E., 2023. Mapping crustal structure and deformation using gravity data in the Bursa Basin

- and surroundings, Türkiye. Turkish Journal of Earth Sciences, 32(7), 7.
- Pašteka R., Karcol R., Kusnirak D., Mojzes A., 2012. REGCONT: a Matlab based program for stable downward continuation of geophysical potential fields using Tikhonov regularization. Comput. Geosci., 49, 278–289.
- Phach P.V., Anh L.D., 2018. Tectonic evolution of the southern part of Central Viet Nam and the adjacent area. Geodyn. Tectonophys., 9(3), 801–825.
- Pham L.T., Oksum E., Do T.D., Huy M.L., 2018. New method for edges detection of magnetic sources using logistic function. Geofizicheskiy Zhurnal, 40(6), 127–135.
- Pham L.T., Van Duong H., Kieu Duy T., Oliveira S.P., Giau L.M., Thanh B.M., Oksum E., 2023. An effective edge detection technique for subsurface structural mapping from potential field data. Acta Geophys., 72, 1661–1674.
- Pham L.T., Oliveira S.P., Le-Huy M., Nguyen D.V., Nguyen-Dang T.Q., Do T.D., Tran K.V., Nguyen H.-D.T., Ngo T.-N.T., Pham H.Q., 2024. Reliable Euler deconvolution solutions of gravity data throughout the β-VDR and THGED methods: application to mineral exploration and geological structural mapping. Vietnam J. Earth Sci., 46(3), 432–448.
- Saada A.S., Eleraki M., Mansour A., Eldosouky A.M., 2025. Insights on the structural framework of the Egyptian Eastern Desert derived from edge detectors of gravity data. Interpretation, 13, T71–T85.
- Sahoo S., Narayan S., Pal S.K., 2022a. Fractal analysis of lineaments using CryoSat-2 and Jason-1 satellitederived gravity data: Evidence of a uniform tectonic activity over the middle part of the Central Indian Ridge. Phys. Chem. Earth, 128, 103237.
- Sahoo S., Narayan S., Pal S.K., 2022b. Appraisal of gravity-based lineaments around Central Indian Ridge (CIR) in different geological periods: Evidence of frequent ridge jumps in the southern block of CIR. J. Asian Earth Sci., 239, 105393.
- Saibi H., Aboud E., Ehara S., 2012a. Analysis and Interpretation of gravity data from the Aluto-Langano geothermal field of Ethiopia. Acta Geophys., 60(2), 318–336.
- Saibi H., Aboud E., Setyawan A., Ehara S., Nishijima J., 2012b. Gravity data analysis of Ungaran volcano, Indonesia. Arab. J. Geosci., 5(5), 1047–1054.

- Sandwell D.T., Muller R.D., Smith W.H.F., Garcia E., Francis R., 2014. New global marine gravity model from CryoSat-2 and Jason-1 reveals buried tectonic structure. Science, 346(6205), 65–67.
- Stewart I.C.F., 2019. A simple approximation for low-latitude magnetic reduction-tothe-pole. J. Appl. Geophys, 166, 57–67.
- Tatchum C.N., Tabod C.T., Koumetio F., Manguelle-Dicoum E., 2011. A gravity model study for differentiating vertical and dipping geological contacts with application to a Bouguer gravity anomaly over the Foumban shear zone, Cameroon. Geophysica, 47(1–2), 43–55.
- Tran K.V., Nguyen T.N., 2020. A novel method for computing the vertical gradients of the potential field: application to downward continuation. Geoph. J. Int., 220(2), 1316–1329.
- Trompat H., Boschetti F., Hornby P., 2003. Improved downward continuation of potential field data. Explor. Geophys, 34(4), 249–256.
- Viet L.T, Tung V.D., Chi V.C., Huong N.T.T., Luan N.V., Nam D.H, Quynh B.V., 2016. Characteristics of fracture zones in Southern Tay Nguyen. Vietnam J Earth Sci, 38(1), 22–37 (in Vietnamese).
- Vu D.T., Bonvalot S., Bruinsma S., Bui L.K., 2021. A local lithospheric structure model for Vietnam derived from a high-resolution gravimetric geoid. Earth Planets Space, 73, 92.
- Wijns C., Perez C., Kowalczyk P., 2005. Theta map: Edge detection in magnetic data. Geophysics, 70, 39–43
- Xu S., Yang J., Yang C., Xiao P., Chen S., Guo Z., 2007. The iteration method for downward continuation of a potential field from a horizontal plane. Geophys. Prospect., 55, 883–889.
- Zhang H., Ravat D., Hu X., 2013. An improved and stable downward continuation of potential field data: the truncated Taylor series iterative downward continuation method, Geophysics, 78(5), J75–J86.
- Zhang C., Lu Q., Yan J., Qi G., 2018. Numerical solutions of the mean-value theorem: New methods for downward continuation of potential fields, Geophys. Res. Lett., 45, 3461–3470.
- Zhang X., Yu P., Tang R., Xiang Y., Zhao C.J., 2015.
 Edge enhancement of potential field data using an enhanced tilt angle. Explor. Geophys., 46(3), 276–283.